RADIO SCIENCE, VOL. 42, RS4025, doi:10.1029/2006RS003544, 2007

Fluctuations of radio occultation signals in X/K band in the presence of anisotropic turbulence and differential transmission retrieval performance

M. E. Gorbunov[1,2] and G. Kirchengast[2]

Received 12 July 2006; revised 28 April 2007; accepted 5 June 2007; published 18 August 2007.

[1] We investigated amplitude fluctuations and differential transmission errors for radio occultation (RO) measurements performed in X/K band for Low-Earth Orbiter – Low-Earth Orbiter (LEO–LEO) cross-links. We performed a series of high-resolution numerical simulations using a quasi-realistic anisotropic turbulence model with European Centre for Medium-Range Weather Forecast (ECMWF) ERA40 reanalyses as the background fields. Three test cases were simulated: high, middle, and low latitudes, with turbulence intensity profile being estimated based on high-resolution radio sonde data. The numerical end-to-end simulations were based on the multiple phase screens technique (forward modeling) and the canonical transform amplitude ratioing method (differential transmission retrieval). The anisotropy coefficient was varied from 3 to 50. We found the dependences of the scintillation index on anisotropy in the area of weak fluctuations to be consistent with previous theoretical studies: scintillation index is approximately proportional to the square root of the anisotropy coefficient. For strong fluctuations this dependence becomes weaker. The type of dependence of differential transmission errors from anisotropy is more sensitive to the fluctuation strength. Generally, it increases with anisotropy, but the dependence saturates for stronger anisotropy and becomes flat or even slightly reverse. At all fluctuation levels, including the strongest ones, the differential transmission error is found smaller than 5% (smaller than 1–2.5% for all weak and moderately strong fluctuations) for ~1 km height resolution, reinforcing the results of the previous studies that X/K band RO phase delay and transmission are a promising future source for accurate temperature and humidity profiling.

Citation: Gorbunov, M. E., and G. Kirchengast (2007), Fluctuations of radio occultation signals in X/K band in the presence of anisotropic turbulence and differential transmission retrieval performance, *Radio Sci.*, *42*, RS4025, doi:10.1029/2006RS003544.

1. Introduction

[2] A system of Low Earth Orbiters (LEOs) equipped with LEO transmitters and LEO receivers of radio signals in the band 8–30 GHz, further referred to as X/K band, is capable of providing wide opportunities for profiling atmospheric temperature, pressure, and humidity [*Kursinski et al.*, 2002; *Lohmann et al.*, 2003b; *Kirchengast et al.*, 2004b, 2004a; *Kirchengast and Høeg*, 2004]. The use of 3 or 4 frequency channels located on the wing of the water vapor absorption line 22.235 GHz allows the retrieval of water vapor from radio occultation (RO) data without any external information. The retrieval is based on the following scheme: (1) the retrieval of bending angle profiles using the Canonical Transform/Full-Spectrum Inversion (CT/FSI) technique [*Gorbunov*, 2002; *Jensen et al.*, 2003; *Gorbunov and Lauritsen*, 2004; *Jensen et al.*, 2004], (2) the Abel inversion of bending angles to the real refractivity profile, (3) the retrieval of integral absorption profiles from the CT/FSI amplitude [*Gorbunov*, 2002; *Lohmann et al.*, 2003a], (4) the Abel inversion of the integral absorption to the imaginary refractivity profile [*Lohmann et al.*, 2003b; *Kirchengast et al.*, 2004b], (5) the retrieval of pressure, temperature, and humidity from the single real refractivity

[1]Institute for Atmospheric Physics, Moscow, Russia.
[2]Wegener Center for Climate and Global Change and Institute for Geophysics, Astrophysics and Meteorology, University of Graz, Graz, Austria.

0048-6604/07/2006RS003544$11.00

profile and multiple imaginary refractivity profiles for the multiple frequency channels [*Kirchengast et al.*, 2004b, 2004a; *Kirchengast and Høeg*, 2004].

[3] Horizontal gradients of atmospheric refractivity and small-scale inhomogeneities are an important source of retrieval errors. In order to reduce these errors, it was suggested to use twin frequencies for the computation of differential transmission [*Kursinski et al.*, 2002; *Facheris and Cuccoli*, 2003]. The effects of scintillations and horizontal gradients should, to a significant extent, cancel out in differential transmission. An important step forward was made by *Gorbunov and Kirchengast* [2005a, 2005b], who introduced a combination of the differential method with CT/FSI retrieval technique. This modification of the differential method results in much better suppression of scintillations due to small-scale turbulence. This conclusion was corroborated by numerical simulations with high-resolution models of anisotropic atmospheric turbulence based on theoretical and experimental investigations [*Gurvich and Brekhovskikh*, 2001; *Gurvich and Chunchuzov*, 2003, 2005; *Fritts and Alexander*, 2003]. A model of turbulence with power spectrum (3D power exponent $\mu_{3D} = -5$) and constant anisotropy coefficient $q = 20$ was employed.

[4] This paper is a continuation of our previous work [*Gorbunov and Kirchengast*, 2005a, 2005b]. We performed high-resolution numerical simulations in order to investigate the dependence of the scintillation index and of differential transmission retrieval errors on the anisotropy coefficient, from large values ($q = 50$) towards almost isotropic turbulence ($q = 3$). In this study we used a decreased internal scale of the turbulence inhomogeneity, which was taken to be 15 m (*Gorbunov and Kirchengast* [2005a, 2005b] used an internal scale of 30 m) and is also below the diffractive limit of about 20 m estimated by *Gorbunov and Kirchengast* [2005b]. This value approaches the typical values of 1–10 m found by *Gurvich and Chunchuzov* [2003], and it lies at the margin of resolution currently feasible in terms of computational expenses.

2. Model

[5] We used a model of the turbulent atmosphere, which includes a regular background part from European Centre for Medium-Range Weather Forecast (ECMWF) ERA40 reanalyses complemented with anisotropic turbulence with a magnitude chosen as estimated from high-resolution (~10 m vertical spacing) radio sonde measurements. The reanalysis fields were given on a latitudinal-longitudinal grid with 0.5° × 0.5° resolution and on 64 vertical levels up to a height of about 60 km. Turbulence was modeled as a random relative perturbation of the refractivity field with a power form of the spectrum:

$$\tilde{B}(\kappa) = \begin{cases} \tilde{c}\kappa_{ext}^{-\mu}, & \kappa < \kappa_{ext} \\ \tilde{c}\kappa^{-\mu}, & \kappa_{ext} \le \kappa \le \kappa_{int} \\ \tilde{c}\kappa^{-\mu} \exp\left[-\left(\dfrac{\kappa - \kappa_{int}}{\kappa_{int}/4}\right)^2\right], & \kappa > \kappa_{int} \end{cases}, \quad (1)$$

where $\kappa = (\kappa_z^2 + q^{2\frac{\kappa_\theta^2}{r_E^2}})^{1/2}$, κ_z and κ_θ are the spatial frequencies (wave numbers) conjugated to the polar coordinates z and θ in the occultation plane (z being the height above the Earth's surface, θ being the polar angle), r_E is the Earth's curvature radius, q is the anisotropy coefficient ($q > 1$, horizontally stretched turbulence). Factor $\tilde{c}$ normalizes the rms turbulent fluctuations to unity. In the coordinate space we use an additional factor $c(z)$, which describes the relative magnitude of turbulent perturbations as a function of altitude. We assumed that the radiosonde-derived fractional refractive index variations are primarily due to turbulence, and we did not model the intermittence of the turbulence. These assumptions can result in an overestimate of the turbulence fluctuation intensity. However, this will be favorable for a conservative (upper-bound oriented) assessment of the method in terms of which transmission retrieval error levels are to be expected.

[6] Our model is based on the theoretical and experimental studies [*Fritts et al.*, 1988; *Fritts and VanZandt*, 1993; *Fritts and Alexander*, 2003; *Gurvich and Brekhovskikh*, 2001; *Gurvich and Chunchuzov*, 2003, 2005]. *Gurvich and Chunchuzov* [2003, 2005] revealed that atmospheric turbulence is a mixture of isotropic (Kolmogorov) component and strongly anisotropic component, which has properties similar to internal gravity waves. We adopted the turbulence to be characterized by an external scale $2\pi/\kappa_{ext} = 100$ m, internal scale $2\pi/\kappa_{int} = 15$ m, exponent $\mu = -4$ for the 2D spectrum (corresponding to exponent $\mu_{3D} = -5$ for the 3D spectrum) that follows [*Gurvich and Chunchuzov*, 2003, 2005]. *Yakovlev et al.* [2003] obtained a close value of $\mu_{3D} = 4.5$.

[7] The value of 100 m for the outer scale of turbulence has been chosen consistent with a parameterized turbulence modeling in previous ACE+ LEO-LEO studies [*Kirchengast et al.*, 2004b, 2004a; *Kirchengast and Høeg*, 2004]. It is a realistic estimate for altitudes 5 to 15 km based on observations of turbulence parameters reported, for example, by *Eaton and Nastrom* [1998] and *Rao et al.* [2001]. The outer scale typically lies around 50–150 m. The internal scale is chosen close to the diffractive limit [*Gorbunov et al.*, 2004]: $h \ge \sqrt[3]{2\lambda^2 r_E}$, which is about 20 m. The effect of adding smaller scales into the amplitude scintillation will be very small due to both the decrease of spectral density of turbulence and diffraction. According to experimental studies [*Kan et*

al., 2002; *Yakovlev et al.*, 1995, 2003], the scales 30–50 m provide about 1% of the total scintillation power. The contribution of the scales below 30 m is accordingly still smaller. Our own sensitivity checks with using 30 m scale instead of 15 m confirm that the contribution of <30 m scales is well below 1%. This indicates that there is safely no need for taking scales below 15 m into account when modeling the propagation of centimeter radio waves. According to *Gurvich and Chunchuzov* [2003, 2005], amplitude fluctuation intensity increases as a function of anisotropy coefficient q until q reaches a value of about 30, where the increase practically saturates. We simulated q equal to 3, 5, 10, 20, and 50, which covers all the characteristic range of q. Whereas anisotropic turbulence is characteristic for stratospheric conditions, one tropospheric example [*Lüdi and Magun*, 2002], which is actually in the boundary layer, indicates that the refractive anisotropy is small for vertical temperature gradients of 0 to −10 K/km, typically encountered in the troposphere. However, a smaller anisotropy results in a smaller scintillation power, therefore, in the latter case our anisotropic model will overestimate scintillations. Our turbulence model results in a realistic pattern of scintillations of the simulated signals looking similar to the experimentally observed ones [*Kan et al.*, 2002; *Yakovlev et al.*, 1995, 2003].

[8] We performed modeling for three cases reflecting regimes of small to large atmospheric turbulence: (1) Lerwick ("high latitude"; 60.2°N, 1.0°W), (2) Gibraltar ("midlatitude"; 36.1°N, 5.3°W), and (3) St. Helena ("low latitude"; 15.6°S, 5.4°W). The rms profiles of relative turbulent fluctuations $c(z)$ were computed upon our request by S. Buehler (University of Bremen, private communication, 2004) on the basis of estimations from high-resolution radio sonde profiles. The profiles are shown in Figure 1, where it is seen that we selected strong turbulence (90% decile) as primary cases.

[9] For modeling the LEO–LEO wave propagation we employed the multiple phase screens technique. We used 2D simulations with 1D phase screens. For the above anisotropy coefficients, the screen-to-screen step was 20, 30, 50, 100, and 200 m, respectively. The vertical discretization step in the screens was 0.2 m. The upper height of the phase screens was 75 km. We used three frequency channels consistent with those baselined for the ACE+ Project [*Kirchengast and Høeg*, 2004]: 9.7 GHz, 17.25 GHz, and 22.6 GHz. We generated one realization of the random perturbation of the refractivity field, using the spectral density defined by (1) and the

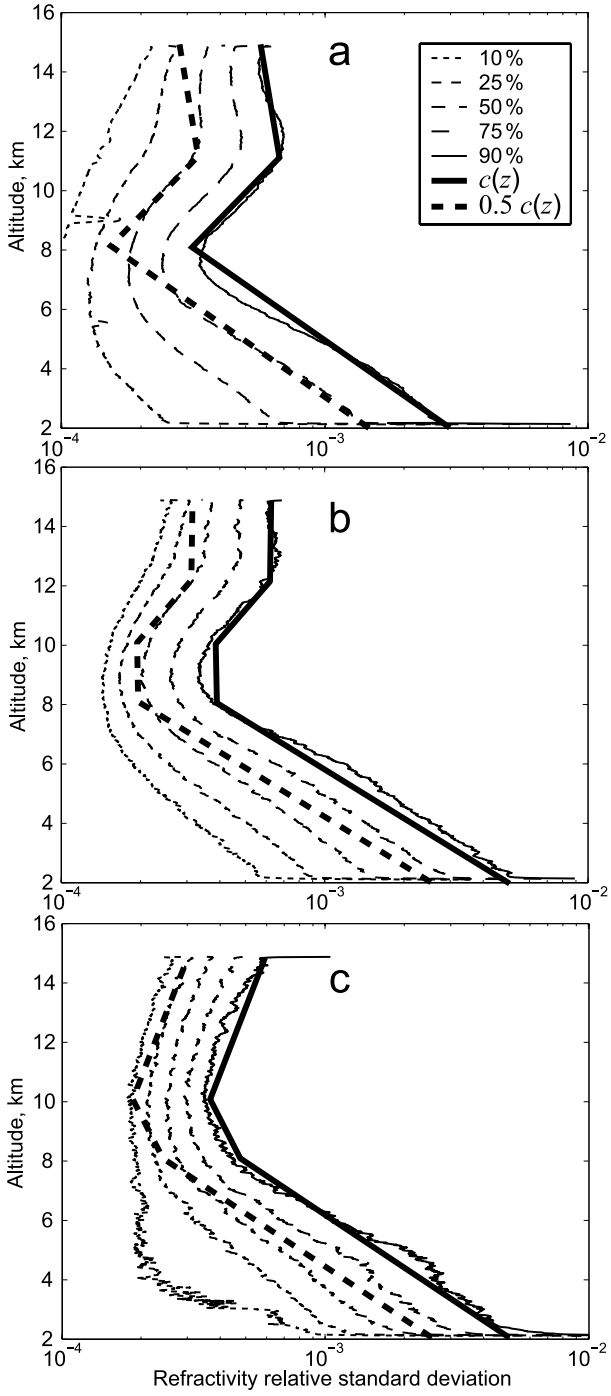

Figure 1. Estimation of rms profiles of turbulent refractivity fluctuations on the basis of hi-res raob profiles observed at (a) Lerwick ("high latitude"; 60.2° N, 1.0° W), (b) Gibraltar ("midlatitude"; 36.1° N, 5.3° W), and (c) St. Helena ("low latitude"; 15.6° S, 5.4° W): Median profile (50%) and different percentiles. The profile "$c(z)$" (heavy black line) reflecting the upper decile - 90% - is primarily used for the turbulence modeling in this study, "$0.5c(z)$" is used as a smaller turbulence reference case. (Original panels by S. Buehler, University of Bremen, Germany; adapted.)

perturbation was superimposed on the background refractivity field taken from a reanalysis of the ECMWF.

[10] This high-resolution forward modeling required an intensive use of computational resources. For example, the simulation of one profile with $q = 3$ and the corresponding screen-to-screen step of 20 m took 20–25 days on a computer system with processor type Pentium-4, 3.0 GHz. This explains why we used a 2D simulation scheme (still quasi-realistic) instead of the full 3D propagation. Furthermore, the Fresnel zone size in the direction transversal to the wave propagation is about 100 m. For $q > 10$, this will be smaller than the horizontal internal scale $2\pi q/\kappa_{int}$ of the modeled atmospheric inhomogeneities, so that the 3rd dimension will not play a relevant role. For $q = 3$ and 5, $2\pi q/\kappa_{int}$ equals 45 m and 75 m, respectively, which will result in neglecting the contribution of the third coordinate into the scintillation power [*Rytov et al.*, 1989], and the 2D restriction will lead to a small underestimate of the scintillation intensity.

[11] In the numerical simulations we computed the wave field $u_j(t; q)$ for each channel j, each anisotropy coefficient q, and each test case (high, mid, low latitude). We also computed the unperturbed fields $u_j^{(0)}(t)$ for the ECMWF atmospheric fields without superimposed turbulence. The corresponding perturbed and unperturbed intensities are $I_j = |u_j|^2$ and $I_j^{(0)} = |u_j^{(0)}|^2$, respectively.

[12] The further processing of the simulated wave fields towards the retrieval of differential transmissions was based on the CT2 technique [*Gorbunov and Lauritsen*, 2004]. The field was mapped into the impact parameter representation by the Fourier Integral Operator (FIO) $\hat{\Phi}_2$. This transform eliminates most of the effects of multipath and diffraction due to the large propagation distance from the planet limb to the observation orbit. The field in the transformed space equals

$$\hat{\Phi}_2 u_j(p) = A_j(p) \exp(ik\Psi(p)), \tag{2}$$

$$A_j(p) = \bar{A}_j K(p) \exp\left(-\tau_j(p)\right), \tag{3}$$

where $\bar{A}_j$ is a normalizing amplitude factor for channel j, $K(p)$ is a geometric optical term that depends on unknown horizontal gradients [*Gorbunov and Kirchengast*, 2005a, 2005b], and $\tau_j(p)$ is logarithmic transmission (or, equivalently, optical thickness). Here we neglect the dependence of the phase $\Psi(p)$ on the frequency channel, because the dispersion of the real refractivity is negligible in X/K band [*Gorbunov and Kirchengast*, 2005b]. Normalizing amplitude factors $\bar{A}_j$ can be determined from the amplitudes at heights 25–30 km, where absorption and the influence of horizontal gradients are negligible. To get rid of the unknown term $K(p)$, *Gorbunov and Kirchengast* [2005a, 2005b] suggested taking the differential transmission between j-th and k-th channels:

$$\tau_{jk} = \tau_j - \tau_k = \ln \frac{A_k(p)/\bar{A}_k}{A_j(p)/\bar{A}_j}. \tag{4}$$

[13] From $\Psi(p)$ we computed the bending angle profile $\epsilon(p)$ and function $t(p)$, the latter denoting the profile of time t as a function of impact parameter p. To this end, we numerically solved the following equation for $t(p)$, using the already defined $\epsilon(p)$:

$$\epsilon(p) = \cos^{-1}\left(\frac{p}{r_T(t)}\right) + \cos^{-1}\left(\frac{p}{r_R(t)}\right) - \theta(t), \tag{5}$$

where $r_{T,R}(t)$ are the transmitter and receiver radii, and $\theta(t)$ is the satellite-to-satellite angular separation in the occultation plane. This allowed for the computation of the logarithmic relative fluctuations of the intensity $\log_{10}(I_j(t(p); q)/I_j^{(0)}(t(p)))$ as well as of the scintillation index:

$$\beta^2 = \left\langle \ln^2\left(\frac{I_j(t(p); q)}{I_j^{(0)}(t(p))}\right)\right\rangle, \tag{6}$$

where the averaging was performed over the following two intervals of ray height $p - r_E$: 5–8 km (strong fluctuations) and 11–14 km (weak fluctuations). In *Rytov et al.* [1989], β^2 is defined as $\langle((I - I^{(0)})/I^{(0)})^2\rangle$. The modified definition is more convenient for strong fluctuations (where the distribution of intensity is approximately lognormal); for weak fluctuations it is close to the original definition. We did not perform averaging below 5 km to exclude fluctuations due to regular multipath and to only operate on turbulent fluctuations.

[14] A theoretical study of the dependence of the turbulent fluctuations from the anisotropy q and the power exponent μ_{3D} was performed by *Gurvich* [1984, 1989] and *Gurvich and Brekhovskikh* [2001] in the framework of weak fluctuation theory. It was shown that the dependence of fluctuation intensity on μ_{3D} is not strong. The intensity curves as functions of anisotropy coefficient for $\mu_{3D} = 10/3$, 11/3, 4, 13/3, and 5 are very close [*Gurvich and Brekhovskikh*, 2001]. We also checked the dependence on internal scale, $2\pi/\kappa_{int}$, within 10 m to 30 m, which was also found weak. Change in the external scale, $2\pi/\kappa_{ext}$, within 100 m to 1 km was investigated by *Gorbunov and Kirchengast* [2005a] yielding a weak influence on differential transmission

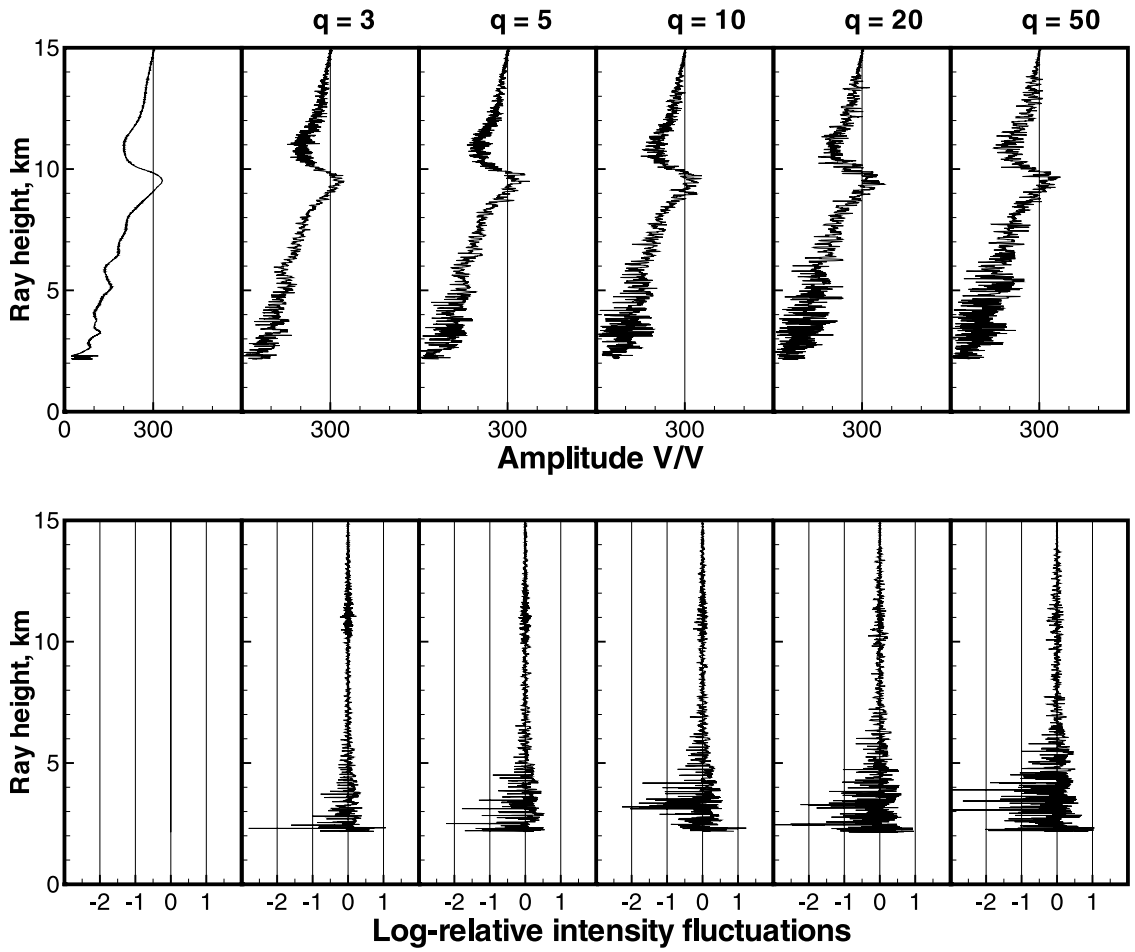

Figure 2. High-latitude case (Lerwick). (top) Amplitudes (V/V) for the channel 1 (9.7 GHz) as function of ray height. Subpanels from left to right: no superimposed turbulence, turbulence with increasing anisotropy coefficient q. (bottom) Plots analogous to the upper panels for log-relative fluctuations of the intensity, where each cell corresponds to an intensity range from $0.001I^{(0)}$ (−3) to $100I^{(0)}$ (+2).

errors. Of primary interest is thus a thorough check of the effect of different anisotropies as discussed below.

3. Numerical Simulation Results

[15] The upper panels of Figures 2, 3, and 4 show amplitudes for the three test cases for the unperturbed atmospheric fields (leftmost subpanel) and the atmosphere with superimposed turbulence with increasing anisotropy coefficient. The lower panels show logarithmic relative fluctuations of the intensity $\log_{10}(I_j(t(p); q)/I_j^{(0)}(t(p)))$. For stronger fluctuations, the distribution of intensity fluctuations begins to deviate from lognormal and becomes asymmetric, drops of amplitudes being more probable than its spikes.

[16] The left panels of Figure 5 show the corresponding average scintillation indices β for ray height range 5–8 km (strong fluctuations) and 11–14 km (weak fluctuations), with $c(z)$ corresponding to strong turbulence (90% decile) in Figure 1. Complementarily, the left panels of Figure 6 show scintillation indices β computed with half as strong turbulence, i.e. following $0.5c(z)$ (roughly representing the 50-percentile). According to *Gurvich and Brekhovskikh* [2001] the scintillation index increases approximately as $q^{1/2}$ for $q < 20$. Our numerical simulations generally confirmed the dependence $\beta \propto q^{1/2}$

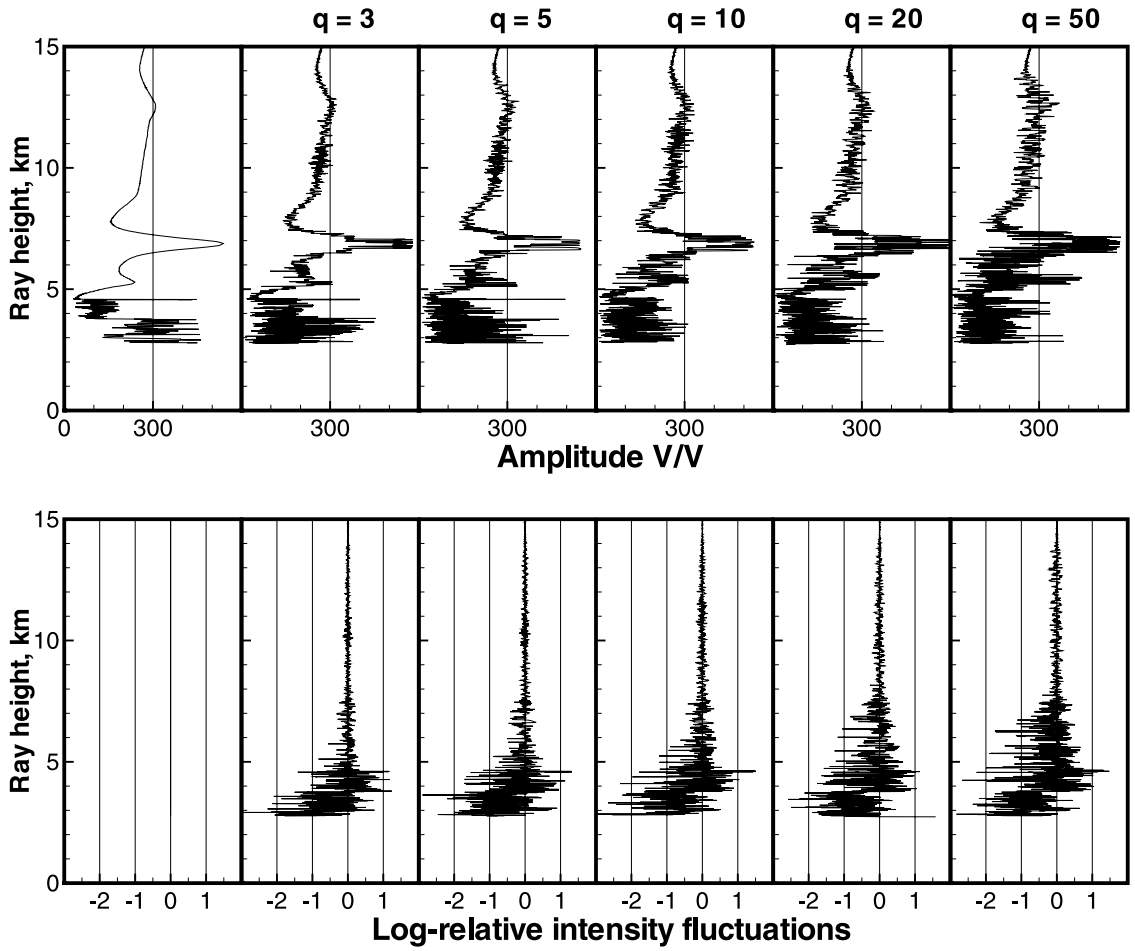

Figure 3. Middle-latitude case (Gibraltar). (top) Amplitudes (V/V) for the channel 1 (9.7 GHz) as function of ray height. Subpanels from left to right: no superimposed turbulence, turbulence with increasing anisotropy coefficient q. (bottom) Plots analogous to the upper panels for log-relative fluctuations of the intensity, where each cell corresponds to an intensity range from $0.001I^{(0)}$ (−3) to $100I^{(0)}$ (+2).

(except for the weakest turbulence, where fluctuations are contaminated with the numerical noise).

[17] The right panels of Figures 5 and 6 show the differential transmission retrieval errors for ∼1 km height resolution (consistent with the ACE+ Project target specifications [*Kirchengast and Høeg*, 2004]). We depict the differential transmission errors between channels 1 (9.7 GHz) and 2 (17.25 GHz). The results are similar for the differential transmission errors between channel 2 and channel 3 (22.6 GHz). Generally, for strong and moderate fluctuations, the differential transmission error as function of q increases for $q < 20$ and saturates or becomes slightly reverse for $q > 20$. For weak fluctuations, it tends to become flat or reverse.

[18] Including receiver noise on realistic level (carrier-to-noise 67 dBHz above atmosphere, ACE+ Mission baseline) does not significantly affect the results at ray heights >5 km, in line with the results of *Gorbunov and Kirchengast* [2005b].

4. Conclusions

[19] We performed high-resolution numerical simulations of radio occultation measurements for a turbulent atmosphere. We used a quasi-realistic anisotropic turbulence model based on previous theoretical and experimental studies and using ECMWF ERA40 global reanalyses as background. Three test cases were investigated: high, mid, and low latitudes, reflecting regimes

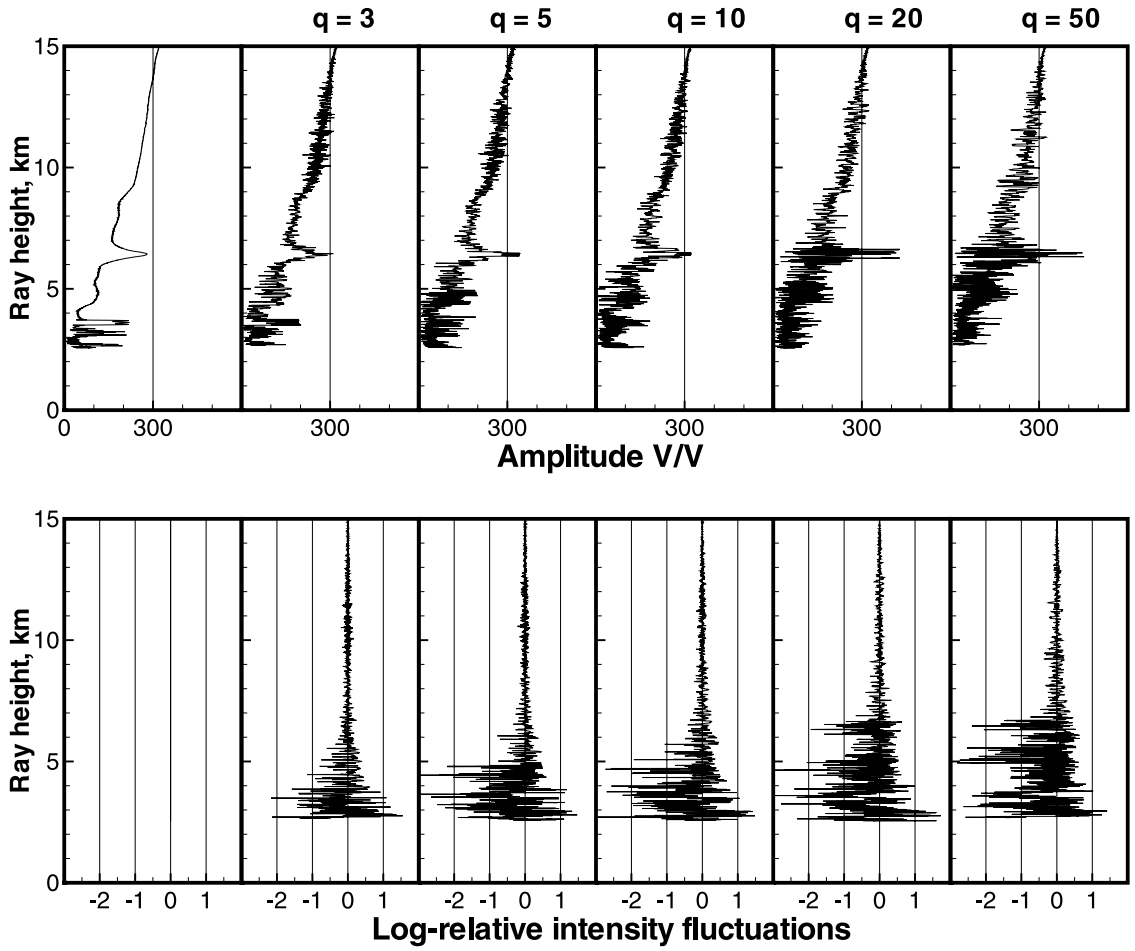

Figure 4. Low-latitude case (St. Helena). (top) Amplitudes (V/V) for the channel 1 (9.7 GHz) as function of ray height. Subpanels from left to right: no superimposed turbulence, turbulence with increasing anisotropy coefficient q. (bottom) Plots analogous to the upper panels for log-relative fluctuations of the intensity, where each cell corresponds to an intensity range from $0.001I^{(0)}$ (-3) to $100I^{(0)}$ $(+2)$.

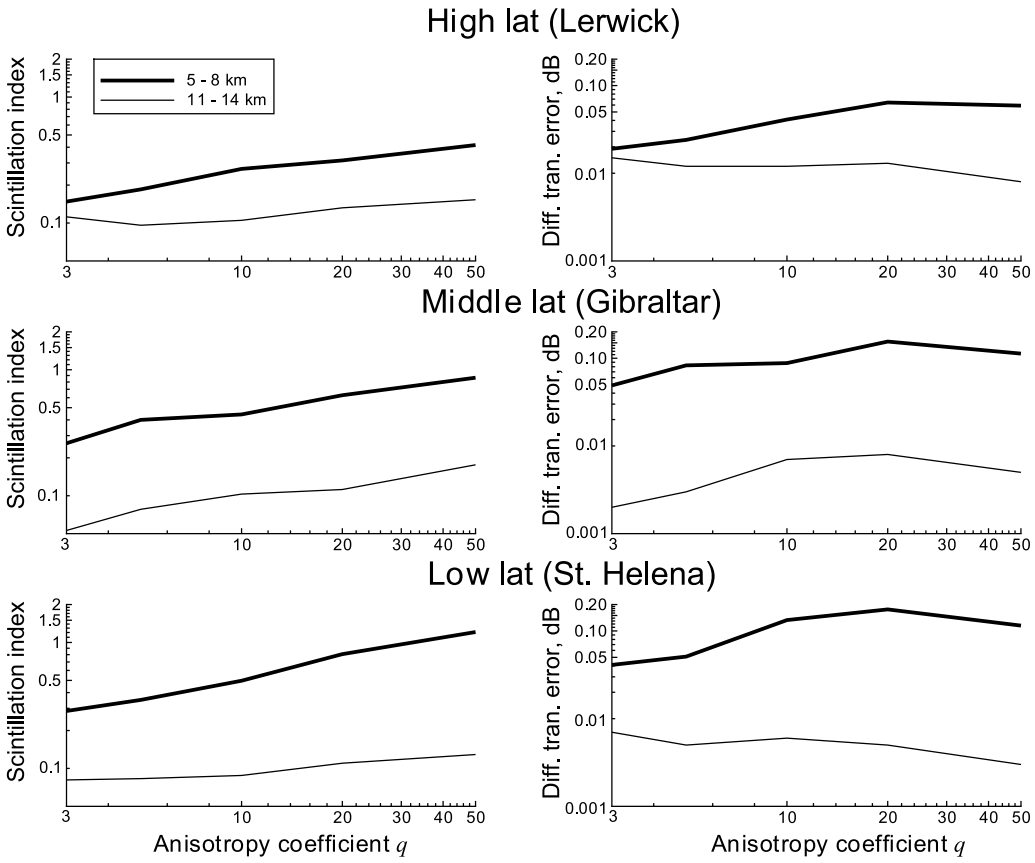

Figure 5. Scintillation index and differential transmission errors (9.7–17.25 GHz channel pair) as functions of anisotropy coefficient for high, mid, and low latitude cases: strong turbulence ("$c(z)$" fluctuation profile).

of weak to strong turbulence. The strength of the turbulence perturbations was taken from high-resolution radio sonde measurements. In particular, we investigated the dependence of amplitude scintillations and differential transmission retrieval errors on the anisotropy coefficient. The dependences of the scintillation index from anisotropy are found generally consistent with previous theoretical studies by *Gurvich and Brekhovskikh* [2001]: scintillation index β is approximately proportional to $q^{1/2}$. This is found to roughly hold also for strong fluctuations, when β exceeds unity. For weak fluctuations the dependence is partly also found weaker and flattened out. The type of dependence of differential transmission retrieval errors from anisotropy is more sensitive to fluctuation strength. Generally, for strong and moderate fluctuations, the differential transmission error increases and saturates or becomes slightly reverse. For weak fluctuations, it tends to become flat or reverse.

[20] At all fluctuation levels the differential transmission error is found <0.2 dB / <5% (<0.05–0.1 dB / <1–2.5% for all weak and moderate level fluctuations) for ~1 km height resolution (multiplication by a factor of $10 \ln 10 \approx 23$ converts units [dB] to [%]). The studies of ACE+ LEO-LEO retrieval performance [*Kirchengast et al.*, 2004b, 2004a; *Kirchengast and Høeg*, 2004] found that noise levels on transmission up to 0.1–0.2 dB lead to accurate temperature and humidity profiling (see also the discussion by *Gorbunov and Kirchengast* [2005a, 2005b]). Our findings in the present paper of differential transmission accuracy better than 0.1–0.2 dB are in line with these requirements. This reinforces the results of previous studies that X/K band radio occultations are a promising method for accurate temperature and humidity profiling in the atmosphere.

[21] Currently, there exist no theoretical strict results to complement the present conclusions on dependence of transmission retrieval errors from anisotropy. A theory describing differential transmission errors in the framework of the CT/FSI method cannot be reasonably based on the thin screen approximation, since for a thin screen

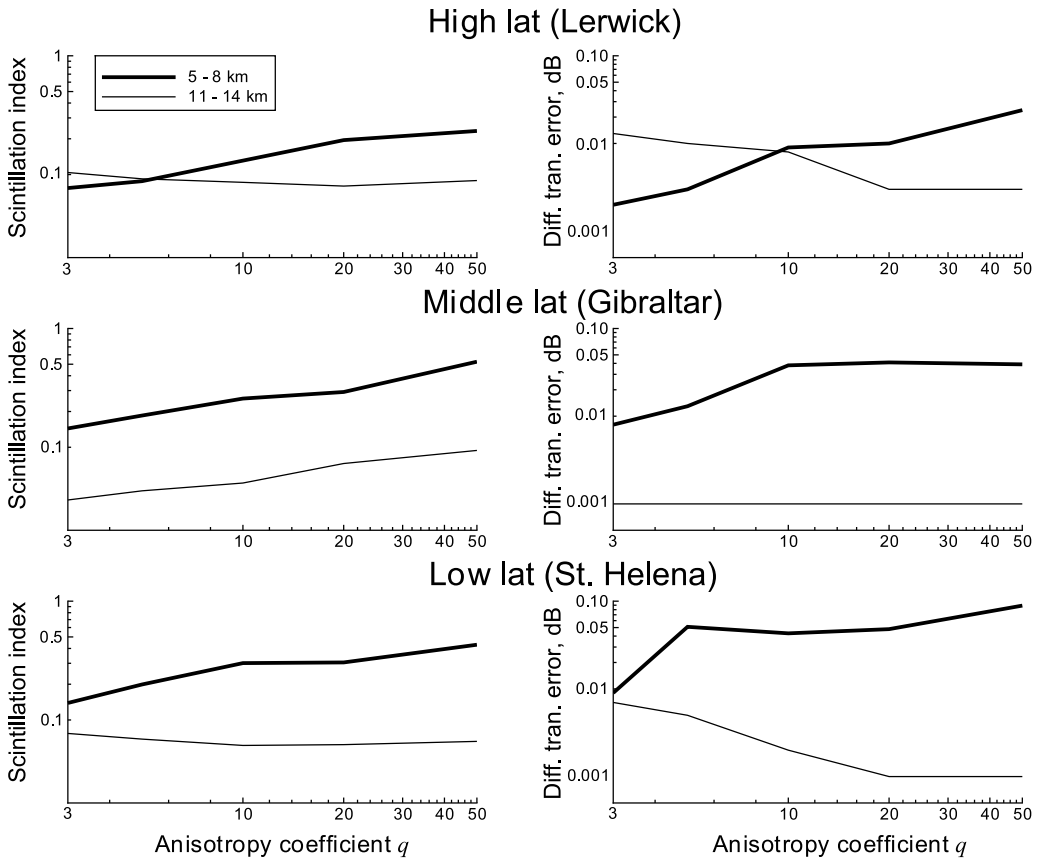

Figure 6. Scintillation index and differential transmission errors (9.7–17.25 GHz channel pair) as functions of anisotropy coefficient for high, mid, and low latitude cases: 50%-reduced turbulence ("$0.5c(z)$" fluctuation profile). The errors are constant (0.001) for the middle latitude case, because 0.001 dB was the numerical accuracy limit of the differential transmission output.

the only error source is the diffraction at the large propagation distance in a vacuum. However, diffraction in a vacuum can be completely canceled out in the CT method, which intrinsically includes back propagation. A theory of the errors of the CT inversion technique should necessarily describe errors due to diffraction on small-scale inhomogeneities inside the turbulent medium. Constructing such a theory is a challenging task.

[22] **Acknowledgments.** The authors gratefully acknowledge valuable discussions related to this work with A. S. Gurvich (Institute for Atmospheric Physics, Moscow, Russia). S. Buehler (University of Bremen, Germany) is thanked for the radio sonde refractivity fluctuation evaluations provided. J. Fritzer and M. Schwärz (Wegener Center, University of Graz, Austria) are thanked for technical and software assistance during the numerical simulations. The work was supported by the Russian Foundation for Basic Research, grant 06-05-64359. The work was funded by the ESA Prodex Arrangement 90152-CN1 (Advanced Topics in RO Modeling and Retrieval Study).

References

Eaton, F. D., and G. D. Nastrom (1998), Preliminary estimates of the vertical profiles of inner and outer scales from white sands missile range, new mexico, VHF radar observations, *Radio Sci.*, *33*, 895.

Facheris, L., and F. Cuccoli (2003), Analysis of differential spectral attenuation measurements applied to a LEO-LEO link, ESA-ACEPASS report (contract 16743/02/NL/FF), Inst. of Elect. and Telecommun., Univ. of Florence.

Fritts, D. C., and M. J. Alexander (2003), Gravity waves dynamics and effects in the middle atmosphere, *Rev. Geophys.*, *41*(1), 1003, doi:10.1029/2001RG000106.

Fritts, D. C., and T. E. VanZandt (1993), Spectral estimates of gravity wave energy and momentum fluxes. part 1: Energy dissipation, acceleration, and constrains, *J. Atmos. Sci.*, *50*, 3685–3694.

Fritts, D. C., T. Tsuda, T. Sato, S. Fukao, and S. Kato (1988), Observational evidence of a saturated gravity wave spectrum in the troposphere and lower stratosphere, *J. Atmos. Sci.*, *45*, 1741–1758.

Gorbunov, M. E. (2002), Canonical transform method for processing GPS radio occultation data in lower troposphere, *Radio Sci.*, *37*(5), 1076, doi:10.1029/2000RS002592.

Gorbunov, M. E., and G. Kirchengast (2005a), Advanced wave-optics processing of LEO-LEO radio occultation data in presence of turbulence, *ESA/ESTEC Tech. Rep. 1/2005*, Univ. of Graz, Austria.

Gorbunov, M. E., and G. Kirchengast (2005b), Processing X/K band radio occultation data in the presence of turbulence, *Radio Sci.*, *40*, RS6001, doi:10.1029/2005RS003263.

Gorbunov, M. E., and K. B. Lauritsen (2004), Analysis of wave fields by Fourier Integral Operators and its application for radio occultations, *Radio Sci.*, *39*, RS4010, doi:10.1029/2003RS002971.

Gorbunov, M. E., H.-H. Benzon, A. S. Jensen, M. S. Lohmann, and A. S. Nielsen (2004), Comparative analysis of radio occultation processing approaches based on Fourier integral operators, *Radio Sci.*, *39*, RS6004, doi:10.1029/2003RS002916.

Gurvich, A. S. (1984), Fluctuations during observations of extraterrestrial sources from space through the atmosphere of the Earth, *Radiophys. Quantum Electron.*, *27*, 665.

Gurvich, A. S. (1989), Scintillation spectra during observations of star obscurations by the Earth's atmosphere, *Atmos. Opt.*, *2*, 188.

Gurvich, A. S., and V. L. Brekhovskikh (2001), Study of the turbulence and inner waves in the stratosphere based on the observations of stellar scintillations from space: A model of scintillation spectra, *Waves in Random Media*, *11*, 163–181.

Gurvich, A. S., and I. P. Chunchuzov (2003), Parameters of the fine density structure in the stratosphere obtained from spacecraft observations of stellar scintillations, *J. Geophys. Res.*, *108*(D5), 4166, doi:10.1029/2002JD002281.

Gurvich, A. S., and I. P. Chunchuzov (2005), Estimates of characteristic scales in the spectrum of internal waves in the stratosphere obtained from space observations of stellar scintillations, *J. Geophys. Res.*, *110*, D03114, doi:10.1029/2004JD005199.

Jensen, A. S., M. S. Lohmann, H.-H. Benzon, and A. S. Nielsen (2003), Full spectrum inversion of radio occultation signals, *Radio Sci.*, *38*(3), 1040, doi:10.1029/2002RS002763.

Jensen, A. S., M. S. Lohmann, A. S. Nielsen, and H.-H. Benzon (2004), Geometrical optics phase matching of radio occultation signals, *Radio Sci.*, *39*, RS3009, doi:10.1029/2003RS002899.

Kan, V., S. S. Matyugov, and O. I. Yakovlev (2002), The structure of stratospheric irregularities according to radio-occultation data obtained using satellite-to-satellite paths, *Izv. VUZ Radiofiz.*, (XLV), 652–663.

Kirchengast, G., and P. Høeg (2004), The ACE+ mission: Atmosphere and climate explorer based on GNSS-LEO and LEO-LEO radio occultation, in *Occultations for Probing Atmosphere and Climate*, edited by G. Kirchengast, U. Foelsche, and A. K. Steiner, pp. 201–220, Springer, Heidelberg.

Kirchengast, G., J. Fritzer, M. Schwaerz, S. Schweitzer, and L. Kornblueh (2004a), The atmosphere and climate explorer mission ACE+: Scientific algorithms and performance overview, *ESA/ESTEC Tech. Rep. 2/2004*, Inst. for Geophys., Astrophys., and Meteorol., Univ. of Graz, Austria.

Kirchengast, G., S. Schweitzer, J. Ramsauer, J. Fritzer, and M. Schwaerz (2004b), Atmospheric profiles retrieved from ACE+ LEO-LEO occultation data: Statistical performance analysis using geometric optics processing, *ESA/ESTEC Tech. Rep. 1/2004*, Inst. for Geophys., Astrophys., and Meteorol., Univ. of Graz, Austria.

Kursinski, E. R., S. Syndergaard, D. Flittner, D. Feng, G. Hajj, B. Herman, D. Ward, and T. Yunck (2002), A microwave occultation observing system optimized to characterize atmospheric water, temperature and geopotential via absorption, *J. Atmos. Oceanic Technol.*, *19*, 1897–1914.

Lohmann, M. S., A. S. Jensen, H.-H. Benzon, and A. S. Nielsen (2003a), Radio occultation retrieval of atmospheric absorption based on FSI, *Sci. Rep. 03-20*, Dan. Meteorol. Inst., Copenhagen.

Lohmann, M. S., L. Olsen, H.-H. Benzon, A. S. Nielsen, A. S. Jensen, and P. Høeg (2003b), Water vapour profiling using LEO-LEO inter-satellite links, in *Proceedings of the Symposium "Atmospheric Remote Sensing Using Satellite Navigation Systems"*, URSI section F/G, Matera, Italy.

Lüdi, A., and A. Magun (2002), Near-horizontal line-of-sight millimeter-wave propagation measurements for the determination of outer length scales and anisotropy of turbulent refractive index fluctuations in the lower troposphere, *Radio Sci.*, *37*(2), 1028, doi:10.1029/2001RS002493.

Rao, D. N., T. N. Rao, M. Venkataratnam, P. Srinivasulu, and P. B. Rao (2001), Diurnal and seasonal variability of turbulence parameters observed with Indian mesosphere-stratosphere-troposphere radar, *Radio Sci.*, *36*, 1439.

Rytov, S. M., Y. A. Kravtsov, and V. Tatarskii (1989), *Principles of Statistical Radiophysics: Wave Propagation Through Random Media*, vol. 4, Springer, New York.

Yakovlev, O. I., S. S. Matyugov, and I. A. Vilkov (1995), Attenuation and scintillation of radio waves in the Earth's atmosphere from radio occultation experiment on satellite-to-satellite links, *Radio Sci.*, *30*, 591–602.

Yakovlev, O. I., S. S. Matyugov, and V. A. Anufriev (2003), Scintillations of centimeter waves and the atmospheric irregularities from radio occultation data, *Radio Sci.*, *38*(2), 1019, doi:10.1029/2000RS002546.

M. E. Gorbunov, Institute for Atmospheric Physics, Pyzhevsky per. 3, Moscow 119017, Russia. (gorbunov@dkrz.de)

G. Kirchengast, Wegener Center for Climate and Global Change, University of Graz (WegCenter/UniGraz), Leechgasse 25, A-8010 Graz, Austria.